International Journal of Earth Sciences Knowledge and Applications
journal homepage: http://www.ijeska.com/index.php/ijeska
e-ISSN: 2687-5993

Research Article https://doi.org/10.5281/zenodo.18076230

# Structural-Geochemical Controls on Mineralization Localization in the Vakijvari Ore Field, Georgia

Giorgi Mindiashvili[1]*, Benjamin Busch[2], David Bluashvili[3], Keti Benashvili[3], Mirian Makadze[1], Revaz Menabde[3], Meri Lekishvili[3]

[1]Ivane Javakhishvili Tbilisi State University, Tbilisi, Georgia
[2]Karlsruhe Institute of Technology, Karlsruhe, Germany
[3]Georgian Technical University, Tbilisi, Georgia

**INFORMATION**

**Article history**
Received 01 October 2025
Revised 20 November 2025
Published 31 December 2025

**Contact**
*Giorgi Mindiashvili
giorgim1994@gmail.com (GM)

**How cite**
Mindiashvili, G., Busch, B., Bluashvili, D., Benashvili, K., Makadze, M., Menabde, R., Lekishvili, M., Bluashvili, D., 2023. Structural-Geochemical Controls on Mineralization Localization in the Vakijvari Ore Field, Georgia. International Journal of Earth Sciences Knowledge and Applications 7 (3), 325-334. https://doi.org/10.5281/zenodo.18076230.

**Abstract**
The Vakijvari Ore Field represents a structurally and geologically complex system formed through multiphase magmatic-hydrothermal processes, genetically linked to the Middle Eocene subvolcanic magmatism of the Adjara-Trialeti rift-fold zone. This study presents an integrated analysis based on petrological, mineralogical, geochemical, and remote sensing data. Microscopic and mineralographic investigations revealed the presence of copper-polymetallic mineralization formed due to fractional crystallization and hydrothermal metasomatism. Using ASTER satellite imagery and DIPS structural analysis software, NE–SW and NW–SE oriented fault systems were identified, which directly control the zoning and localization of mineralization. The integrated dataset demonstrates that structural control, magmatic evolution, and late-stage hydrothermal alteration collectively drive ore body formation, establishing the Vakijvari Ore Field as a significant target for future geological and mineral resource exploration and evaluation.

**Keywords**
Hydrothermal alteration, ore field, intrusive rocks, rift-related magmatism, structural control

## 1. Introduction

The Vakijvari Ore Field represents one of the metallogenic segments within the Lesser Caucasus and is situated in the Middle Eocene volcanic–plutonic complex of the Achara–Trialeti rift–fold zone (Adamia et al., 2011; Okrostsvaridze et al., 2020) (Fig. 1). Briefly emphasizing the economic and geodynamic significance of the Vakijvari field within the regional magmatic arc system further strengthens the introduction. This zone is geodynamically characterized by the development of intensive subvolcanic intrusions and widespread mineralization, which together create favorable conditions for hydrothermal and metasomatic processes (White and Hedenquist, 1995; Cooke et al., 2011).

This study aims to deliver a comprehensive and integrated characterization of the structural–geological framework, magmatic and hydrothermal evolution, and ore-forming processes within the Vakijvari Ore Field. To strengthen the scientific originality of the research, the study explicitly emphasizes its novel contribution: the integration of newly generated geochemical datasets with detailed petrographic observations, systematic structural measurements, and satellite-based lineament analysis. This combined approach provides a more holistic understanding of the factors controlling mineralization than previously available for the region. The methodological design of the research consists of three mutually reinforcing analytical components.

1. Petrographic and mineralogical analysis, documenting magmatic differentiation pathways and metasomatic

overprinting within the intrusive rocks, thereby offering insights into melt evolution and fluid–rock interaction (Audétat et al., 2000; Frost et al., 2001),
2. Structural–geological analysis, based on systematic field measurements of fault orientations, deformation intensities, and fracture networks, followed by quantitative stereographic and cluster-based interpretation using DIPS software (Sibson, 1996; Faulds and Varga, 1998),
3. Remote sensing analysis, using Terra ASTER multispectral data to delineate lineament patterns, vegetation contrasts, and surface morphological variations that reflect underlying structural trends (Gillespie et al., 1987; Rowan et al., 2005).

This approach is grounded in the hypothesis that intrusive bodies genetically linked to continental rift–related magmatism (Bonin, 2004; Okrostsvaridze et al., 2014) play a fundamental role in initiating magmatic differentiation and generating fluid activity (Audétat et al., 2000; Chiaradia, 2009). At the same time, fault–intersection zones act as structural conduits that localize hydrothermal fluid flow and concentrate mineralization (Sibson, 1996; Faulds and Varga, 1998).

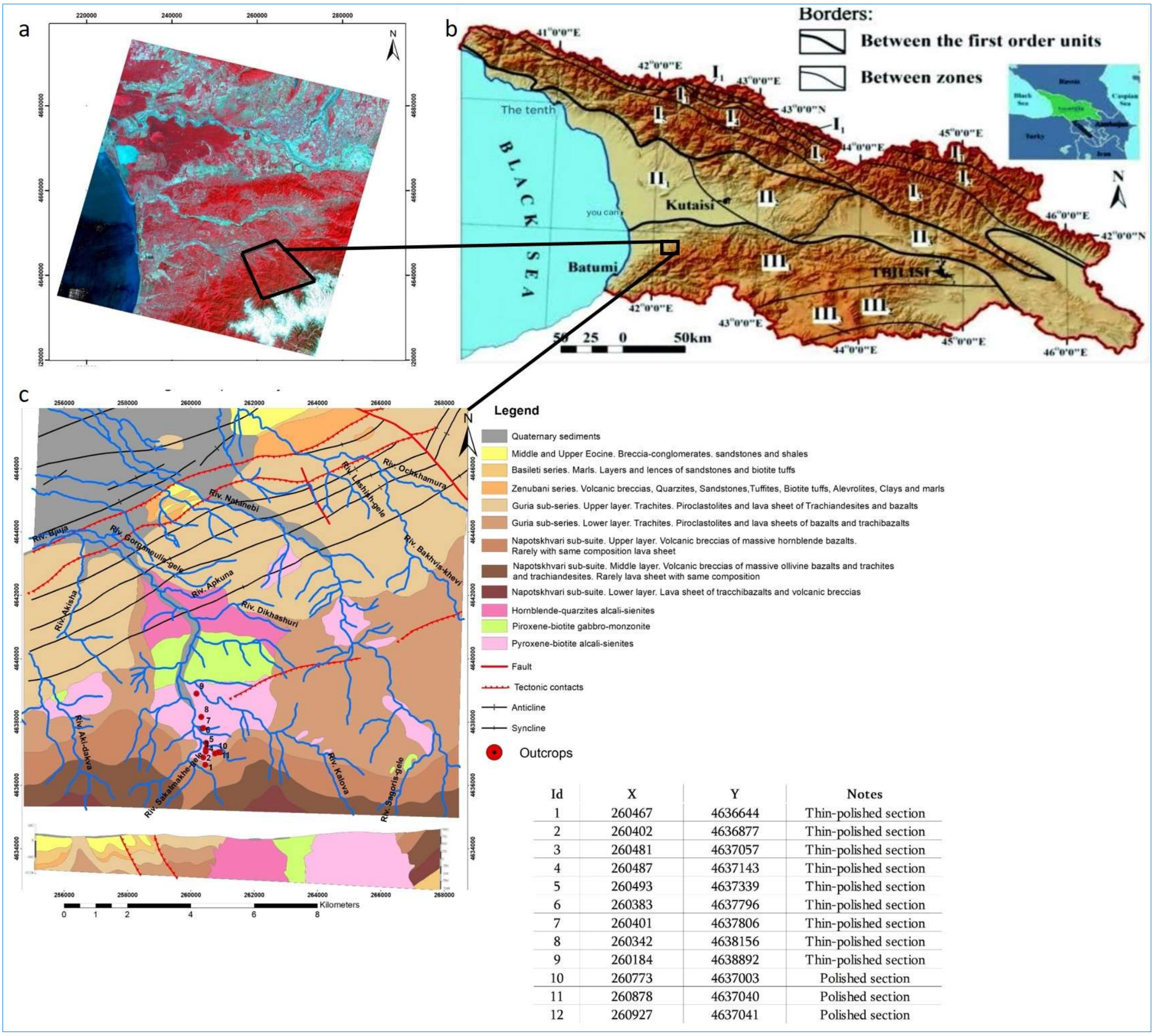


| Id | X | Y | Notes |
|---|---|---|---|
| 1 | 260467 | 4636644 | Thin-polished section |
| 2 | 260402 | 4636877 | Thin-polished section |
| 3 | 260481 | 4637057 | Thin-polished section |
| 4 | 260487 | 4637143 | Thin-polished section |
| 5 | 260493 | 4637339 | Thin-polished section |
| 6 | 260383 | 4637796 | Thin-polished section |
| 7 | 260401 | 4637806 | Thin-polished section |
| 8 | 260342 | 4638156 | Thin-polished section |
| 9 | 260184 | 4638892 | Thin-polished section |
| 10 | 260773 | 4637003 | Polished section |
| 11 | 260878 | 4637040 | Polished section |
| 12 | 260927 | 4637041 | Polished section |

Fig. 1. (a) Terra ASTER 3-2-1 (RGB) composite image of the Vakijvari Ore Field and its surrounding area, (b) Geological structure of Georgia (modified after Gamkrelidze et al., 2020) and (c) Geological map of the Vakijvari Ore Field (modified after Chkhikvishvili, 1992)

Accordingly, the Vakijvari Ore Field represents a classic example of the multiphase interaction of magmatic, structural, and hydrothermal processes. Its investigation is not only scientifically significant for refining regional metallogenic models but also economically relevant, as the field hosts copper–polymetallic mineralization characteristic of the Lesser Caucasus metallogenic province.

## 2. Method of Study

The geological structure and mineralization mechanisms of the Vakijvari ore field were investigated using an integrated methodological framework that combines petrographic–mineralogical studies, structural–geological analysis, remote sensing data, and geochemical interpretation. The emphasis on integration is strengthened by explicitly outlining how each methodological component is interconnected: sampling was conducted according to lithological and structural criteria, petrographic and geochemical analyses provided mineralogical and compositional constraints, and structural and remote sensing datasets were jointly used to interpret the spatial organisation of mineralization. Together, these components form a coherent analytical system for understanding the spatial, genetic, and structural controls on ore formation.

Table 1. Major element oxide composition (wt%) of intrusive rocks from the Guria Region

| Sample_ID | SiO2 | TiO2 | Al2O3 | Fe2O3 | FeO | MnO | MgO | CaO | Na2O | K2O | P2O5 |
|---|---|---|---|---|---|---|---|---|---|---|---|
| SD-1 | 61,88 | 1 | 15,14 | 3,52 | 4,26 | -0,04 | 2,74 | 3,87 | 3,92 | 3,02 | 0,19 |
| SD-2 | 56,78 | 0,65 | 17,5 | 3,76 | 2,64 | 0,17 | 3,3 | 5,98 | 4,19 | 3,43 | 0,17 |
| SD-3 | 58,51 | 0,55 | 15,91 | 2,87 | 3,8 | -0,01 | 4,83 | 4,25 | 4,47 | 4,07 | 0,23 |
| SD-4 | 59,3 | 1,05 | 16,69 | 3,29 | 4,04 | 0,21 | 3,31 | 3,66 | 4,12 | 3,46 | 0,34 |
| SD-5 | 59,66 | 1,12 | 15,08 | 3,12 | 4,68 | -0,01 | 3,05 | 5,97 | 3,67 | 2,8 | 0,05 |
| SD-6 | 60,03 | 0,73 | 15,36 | 3,12 | 3,09 | 0,25 | 3,41 | 4,52 | 4,69 | 3,94 | 0,25 |
| SD-7 | 60,08 | 0,58 | 15,61 | 2,4 | 3,52 | 0,24 | 2,27 | 6,27 | 4,2 | 3,72 | 0,18 |
| SD-8 | 61,99 | 1,19 | 15,19 | 3,63 | 2,55 | -0,04 | 2,26 | 5,56 | 3,48 | 3,04 | 0,25 |

Table 2. Structural Measurements of Joints and Faults in the Guria Region Based on DIPS Analysis. The current version of the table provides essential structural data; however, its interpretive value would be substantially improved by adding additional descriptive columns. In particular, including the geographic coordinates of each observation point, the lithological unit at each site, the fault or fracture type (e.g., normal, reverse, strike-slip, tension joint, shear fracture), and the associated alteration type (e.g., sericitic, chloritic, silicic alteration) would make the dataset more comprehensive

| Dip | Dip-dir | N | Freq |
|---|---|---|---|
| 45 | 245 | Joint | 7 |
| 85 | 0 | Joint | 10 |
| 50 | 200 | Joint | 15 |
| 85 | 0 | Fault | |
| 60 | 0 | Fault | |
| 80 | 5 | Joint | 20 |
| 15 | 0 | Joint | 9 |
| 55 | 210 | Joint | 7 |
| 85 | 0 | Fault | |
| 50 | 160 | Fault | |
| 85 | 0 | Joint | 18 |
| 80 | 10 | Joint | 15 |
| 80 | 180 | Joint | 8 |
| 50 | 85 | Fault | |
| 85 | 15 | Joint | 9 |
| 65 | 280 | Joint | 10 |
| 70 | 230 | Joint | 17 |
| 85 | 250 | Fault | |
| 85 | 250 | Joint | 17 |
| 60 | 240 | Joint | 16 |
| 50 | 175 | Joint | 8 |
| 85 | 0 | Joint | 10 |
| 65 | 45 | Joint | 10 |
| 75 | 170 | Joint | 7 |
| 85 | 0 | Joint | 12 |
| 60 | 50 | Joint | 7 |
| 45 | 50 | Joint | 8 |
| 55 | 170 | Joint | 12 |
| 75 | 10 | Joint | 8 |
| 70 | 110 | Joint | 7 |
| 85 | 190 | Joint | 5 |
| 85 | 10 | Joint | 8 |
| 70 | 110 | Joint | 6 |
| 60 | 190 | Joint | 4 |

The first stage of the investigation involved detailed microscopic analysis of subvolcanic intrusive rocks from Vakijvari, performed at the Karlsruhe Institute of Technology. Fourteen samples were collected from representative lithologies, including monzodiorite, quartz–monzonite and dioritic subvolcanic bodies, to document their mineralogical composition, textural evolution, and hydrothermal overprinting. Petrographic observations were conducted under plane-polarized and cross-polarized light, enabling the identification of magmatic textures, mineral assemblages, and metasomatic transformations (Audétat et al., 2000; Sillitoe, 2010).

Key indicators of fractional crystallization-such as zoned plagioclase, hypidiomorphic granular textures, and variable mafic mineral proportions were recorded, along with evidence of hydrothermal alteration including sericitization, chloritization, silicification, and partial argillic replacement (Frost et al., 2001; Chiaradia, 2009).

Sulfide mineralization was examined with emphasis on mineral associations, textural relationships, and paragenetic development. The identified assemblages—pyrite ($FeS_2$), chalcopyrite ($CuFeS_2$), magnetite, sphalerite, and galena—are characteristic of porphyry-type Cu–Cu-polymetallic systems (Sillitoe, 2010). Both hypogene and supergene stages were documented, including brecciation textures, veinlet networks, late-stage mineral overprinting, and oxidation-related transformations.

XRF geochemical analyses were carried out on selected samples (Table 1). For improved methodological transparency, it is essential to specify the laboratory conditions, instrument model, analytical precision and accuracy, and reference standards used (e.g., USGS rock standards such as AGV-2, BHVO-2). Major-element data were interpreted using a series of standard geochemical diagrams.

TAS classification diagrams (Middlemost, 1994; Cox et al., 1979) were employed to distinguish igneous rock types; however, because Na and K are susceptible to hydrothermal mobility, the alteration status of the samples must be taken into consideration when interpreting TAS results. Magmatic series were determined using AFM diagrams to distinguish calc-alkaline trends (Frost et al., 2001). Shand's index and Frost's parameters were used to classify metaluminous versus peraluminous character (Shand, 1927; Frost et al., 2001).

Binary variation diagrams for major oxides ($Al_2O_3$, MgO, FeO, CaO, $K_2O$) provided insights into fractional crystallization, magma differentiation, and the superimposed effects of hydrothermal alteration (Rollinson, 1993).

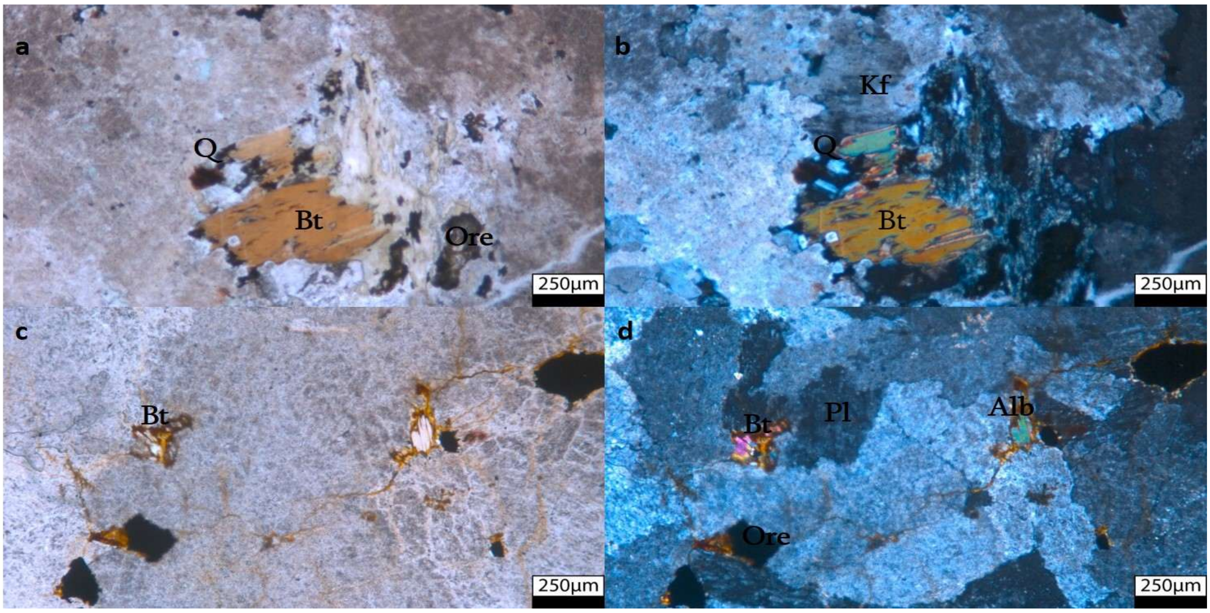


Fig. 2. Magmatic mineralogical associations of the Vakijvari intrusive rocks. Mineral abbreviations: Pl – plagioclase, Qz – quartz, Bt – biotite, Kfs – K-feldspar, Chl – chlorite, Ser – sericite. All thin-section images are shown under specified optical conditions (PPL – plane-polarized light; XPL – cross-polarized light), indicating whether the analyzer is inserted or removed

Within the Vakijvari intrusive complex, nine primary structural observation points were selected during fieldwork (Table 2). The selection of these sites was based on clearly defined criteria, including:

1) lithological representativeness (monzodiorite, quartz–monzonite, and associated subvolcanic units);
2) structural intensity, such as high fracture density, visible fault intersections, or evidence of brittle deformation;
3) presence of mineralization indicators, including sulfide veinlets, iron-oxide staining, or alteration halos; and
4) accessibility and exposure quality, ensuring reliable measurement conditions.

Specifying these criteria provides a stronger scientific justification for the field-sampling strategy.

All structural measurements were processed using the DIPS structural-analysis software. In total, n = 127 fracture and fault-plane measurements were evaluated. The analysis included:

1) equal-area lower-hemisphere stereonet plots and
2) pole-density contour diagrams,

K-means cluster grouping, where k = 3 was selected based on data dispersion, and evaluation of the spatial distribution of major structural families relevant to fluid migration and mineralization (Sibson, 1996; Faulds and Varga, 1998).

Analysis. The current version of the table provides essential structural data; however, its interpretive value would be substantially improved by adding additional descriptive columns. In particular, including the geographic coordinates of each observation point, the lithological unit at each site, the fault or fracture type (e.g., normal, reverse, strike-slip, tension joint, shear fracture), and the associated alteration type (e.g., sericitic, chloritic, silicic alteration) would make the dataset more comprehensive.

Remote sensing analysis was conducted using Terra ASTER satellite imagery, and to ensure methodological transparency and reproducibility, it is essential to specify the software environment and preprocessing workflow applied during data processing. In this study, image analysis was performed using ENVI 5.x and ArcGIS Pro, following standard preprocessing steps including geometric correction, cloud and vegetation masking using NDVI, radiometric calibration, and application of edge-enhancement filters to highlight structural discontinuities.

The following ASTER datasets were utilized:

- AST_L1B – radiometrically calibrated VNIR/SWIR imagery;
- AST_07XT – atmospherically corrected surface reflectance data;
- AST_L1T – terrain-corrected TIR (thermal infrared) bands for detecting thermal anomalies.

Several composite images were generated, including RGB (3-2-1) natural-color scenes and stereoscopic (2-1-1) combinations. These visualizations clearly revealed:

- Prominent NE–SW and NW–SE oriented lineament structures,

- Thermal and reflectance anomalies associated with hydrothermal alteration zones,

Structural nodes that spatially correspond to mineralized sites (Rowan et al., 2005; Gillespie et al., 1987).

## 3. Results

The integrated study of the Vakijvari ore field demonstrates that the system represents a complex magmatic–hydrothermal, structural–petrological unit, where the spatial localization of mineralization is controlled by fractional crystallization, late-stage hydrothermal metasomatism, and the geometry of fault systems and their intersection zones.
Microscopic analysis (Fig. 2) shows that the plutonic rocks are dominated by a biotite–quartz–feldspar mineral assemblage. Hypidiomorphic textures and medium-grained structures indicate relatively slow magma crystallization. Zoned plagioclase, biotite crystals, and undulatory extinction in quartz reflect progressive magmatic differentiation and subsequent deformation processes.

Multiphase hydrothermal alteration is evident through sericitization, chloritization, kaolinitization, and localized concentrations of iron oxides (Fig. 3). Sericite extensively replaces plagioclase, while biotite is altered to chlorite, indicating low-temperature hydrothermal conditions. Kaolinite and montmorillonite development is mainly restricted to secondary alteration zones.

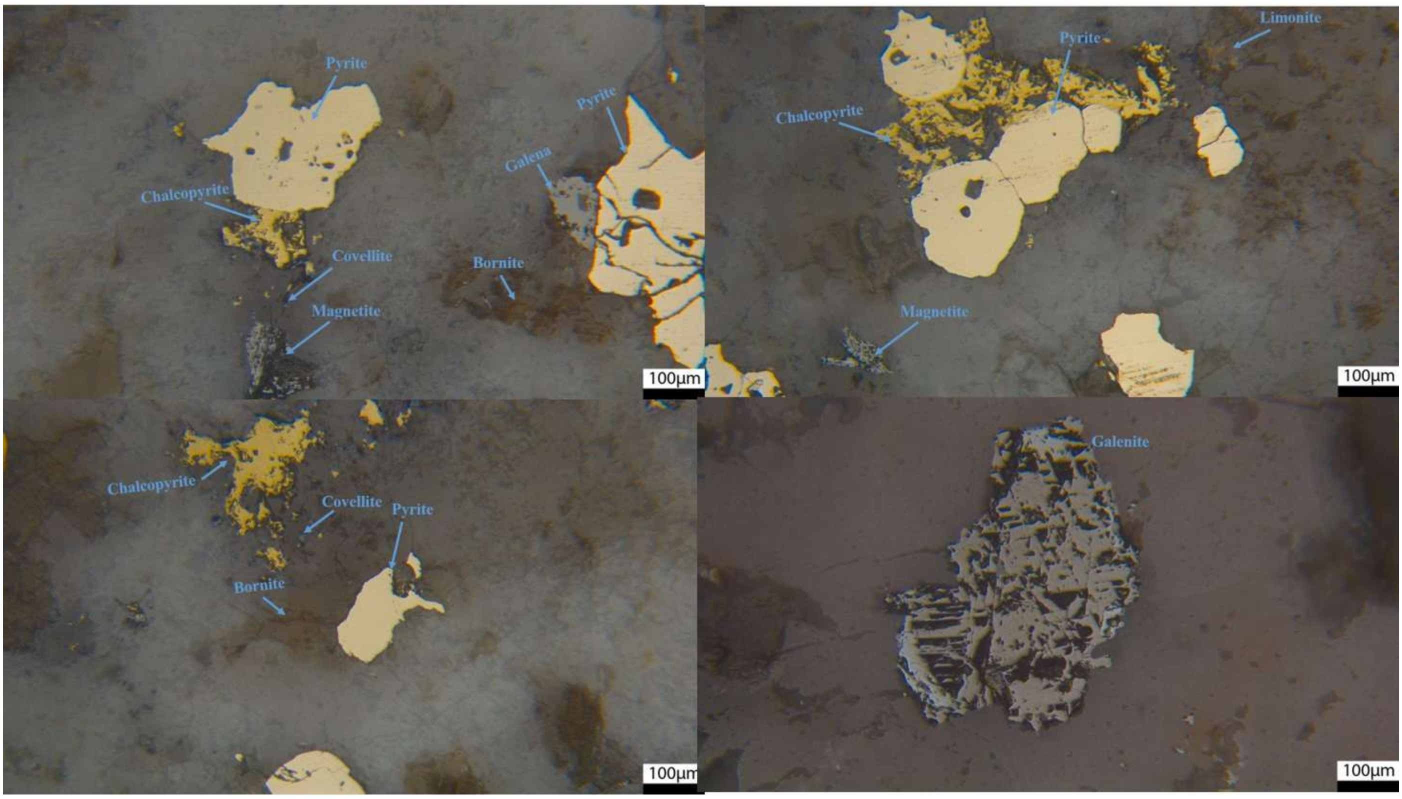


Fig. 4. Ore minerals in a microscope image

Microscopic analysis also revealed ore mineral associations typical of porphyry-style systems (Fig. 4), including pyrite, chalcopyrite, bornite, covellite, magnetite, and galena. The mineral assemblage, together with sulfide zonation patterns, indicates a Cu–Pb–Zn–type porphyry system. Chalcopyrite and pyrite occur in both euhedral and anhedral forms, while the partial replacement of bornite by covellite reflects supergene overprinting. Magnetite is present within secondary vein structures, suggesting a hydrothermal origin.

Geochemical analyses (Fig. 5) show that the investigated intrusive rocks plot within the monzodiorite and quartz monzonite fields in the TAS plutonic classification diagrams (a–b). Two published TAS schemes were used for comparison to ensure consistency, although applying a single standard classification would yield the same lithological interpretation. The samples belong to the calc-alkaline magmatic series (AFM, d) and display a metaluminous to weakly peraluminous character (Al-saturation index, c).

The geochemical pattern derived from the major oxides indicates that magmatic differentiation was largely controlled by fractional crystallization. This is reflected in the moderate $SiO_2$ contents, decreasing MgO and Mg, and systematic variations in FeO*, CaO, and alkali elements, which together suggest evolution from a moderately mafic parent magma toward more evolved intermediate–felsic compositions.

Binary variation diagrams (Fig. 6) demonstrate systematic geochemical trends in the Vakijvari intrusive rocks. The major oxides MgO, CaO, MnO, $Na_2O$, and $K_2O$ show a pronounced negative correlation with $SiO_2$, reflecting progressively evolved magma compositions. These trends are consistent with the fractional crystallization of plagioclase and ferromagnesian minerals, which selectively remove Mg, Ca, Fe, and alkalis from the melt. In addition, $TiO_2$ and MnO also decrease with increasing $SiO_2$, indicating the fractionation of Fe–Ti oxides and mafic silicates during magma evolution. $Al_2O_3$, by contrast, exhibits a more subdued or near-constant relationship with $SiO_2$, reflecting the stabilization of intermediate plagioclase compositions rather than strong fractionation-driven depletion.

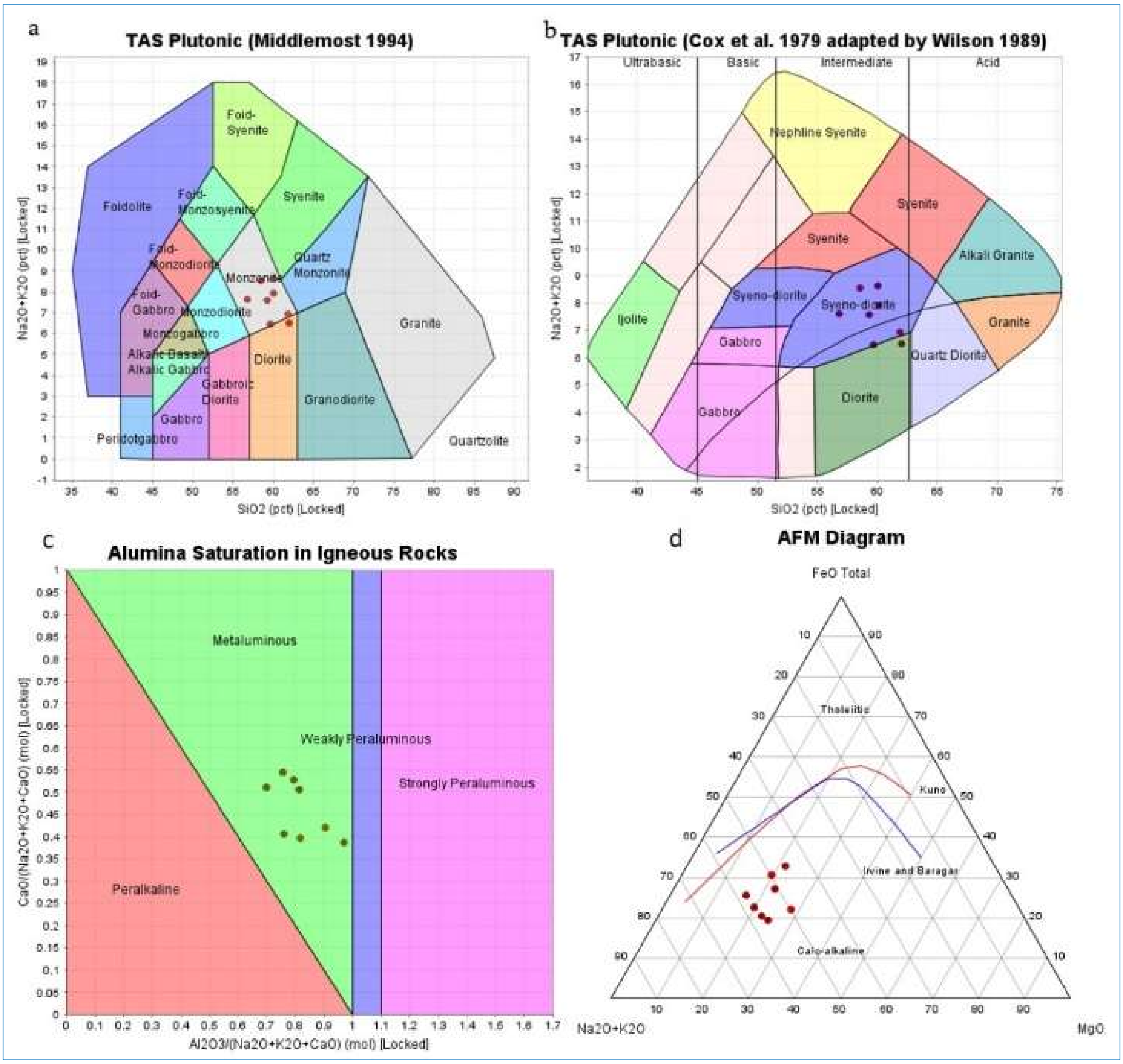


Fig. 5. Geochemical classification of samples

The integration of remote sensing data with field measurements processed in DIPS reveals two dominant lineament sets in the Vakijvari area (Figs. 7a–c). The primary NE–ENE–SW-trending deep-seated faults act as major conduits for ascending hydrothermal fluids, while the secondary NW–SE structures intersect these principal faults to form structural nodes that are particularly favorable for mineralization localization.

High-density domains identified on the polar and rose diagrams correspond closely with field-verified sites where microscopic and mineralographic analyses document intense hydrothermal alteration and the concentration of ore minerals.

## 4. Discussion

Petrological, mineralogical, geochemical, and structural-geological data obtained from the Vakijvari ore field collectively suggest that the intrusive and hydrothermal system likely developed within an intracontinental extensional regime active in the Achara–Trialeti domain since the Middle Eocene (Adamia et al., 2010; Sosson et al., 2010).

Because the present interpretation relies primarily on major oxide geochemistry, it should be regarded as a preliminary geodynamic model. The intracontinental rift setting could be further strengthened in future studies by integrating regional geochronological constraints, extensional fault kinematics, or structural markers that document contemporaneous rifting in the Achara–Trialeti zone. Nevertheless, the proposed interpretation aligns with global observations that link magmatic–hydrothermal systems to post-collisional or intraplate extensional environments, characterized by episodic magmatism, open fracture networks, and multiphase hydrothermal activity (Moritz et al., 2006).

The intrusive rocks of Vakijvari exhibit a calc-alkaline, metaluminous to weakly peraluminous, and moderately alkaline composition, consistent with magmatic products generated during decompression melting in an extensional crustal setting (Wilson, 1989; McKenzie and Bickle, 1988; Bonin, 2004). Although the study does not include a multi-element variation diagram, the available major-oxide chemistry does not indicate classic subduction-related signatures such as strong Nb–Ta depletion or a negative Th–Nb anomaly (Pearce, 1996).

While the absence of such anomalies is compatible with a rift-related or post-collisional setting, it should be noted that similar geochemical traits can also appear in late- to post-collisional arc systems; acknowledging this complexity prevents overgeneralization of the tectonic environment.

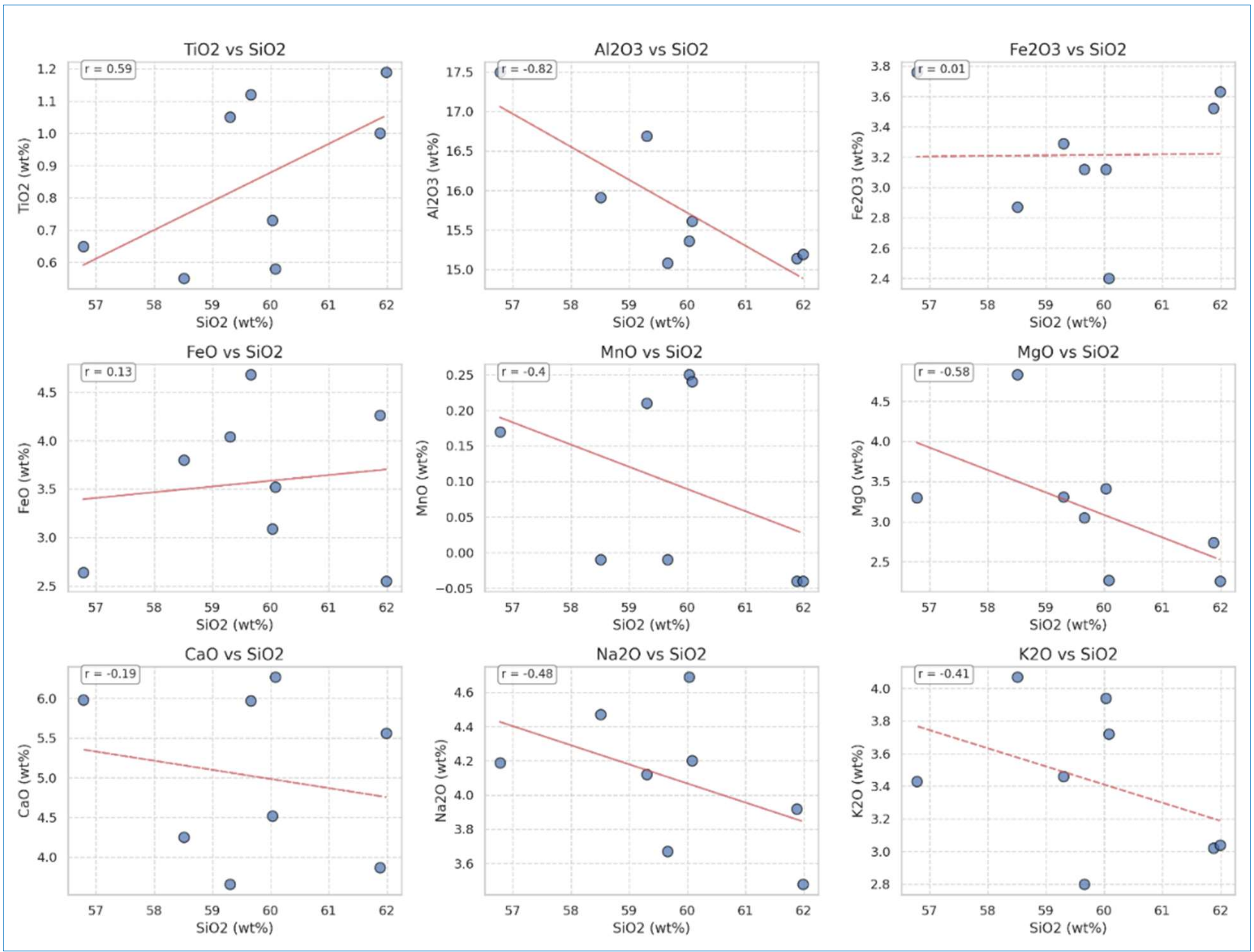


Fig. 6. Binary variation diagrams

The negative correlations of MgO, CaO, FeO, and other compatible elements with increasing $SiO_2$ indicate progressive fractional crystallization of low-Mg, water-rich magmas (Chiaradia, 2009; Sisson and Grove, 1993).

Such melts are capable of exsolving aqueous fluid phases at moderate crustal depths, generating characteristic phyllic, argillic, and propylitic alteration zones commonly associated with porphyry-type mineral systems (White and Hedenquist, 1995; Sillitoe, 2010).

Microscopic observations confirm this pattern through the development of sericitization, chloritization, and kaolinization. The estimated alteration temperatures (~200–350 °C) are inferred from mineral assemblage analogues reported in global porphyry systems, as direct fluid inclusion data were not obtained in this study. Clarifying the origin of these temperature constraints strengthens the reliability of this interpretation.

Structural data further support an extensional environment. The principal NE–ENE–SW-trending fault systems, intersected by secondary NW–SE structures, correspond to typical rift-related fracture geometries (Sibson, 1996; Faulds and Varga, 1998). These intersection zones form structural nodes where permeability is enhanced and pressure-drop conditions develop, facilitating focused hydrothermal flow and metal deposition. Field observations and DIPS analyses show that these structural intersections coincide with zones of intensive alteration and mineralization. Comparable relationships between fault-controlled fluid pathways and mineralization have been documented in post-collisional Cu–Au systems of Argentina (Bissig and Tosdal, 2009) and Iran (Jebelli and Yousefi, 2022); including these analogues enhances the regional relevance of the Vakijvari Model.

Remote sensing data derived from ASTER 211 stereo composites reveal a highly segmented lineament network consistent with a tectonically heterogeneous rift domain.

The spatial arrangement of magmatic centers, alteration zones, and structural intersections fits well with the geometric model proposed by Ghasemi and Talbot (2006), whereby magmatic-hydrothermal activity within rift segments is strongly controlled by the inherited structural fabric.

Ore mineral associations in the Vakijvari field–pyrite, chalcopyrite, bornite, covellite, and magnetite–are indicative of multiphase copper–polymetallic mineralization generated by cooling calc-alkaline intrusions. Their occurrence in both magmatic and hydrothermal vein networks aligns with fluid-driven mineralization processes typical of porphyry systems (Audétat et al., 2000; Richards, 2005).

The coexistence of magmatic and hydrothermal sulfides further supports a model in which metal deposition was governed by structurally focused fluid circulation and prolonged magmatic–hydrothermal evolution in an extensional geological environment.

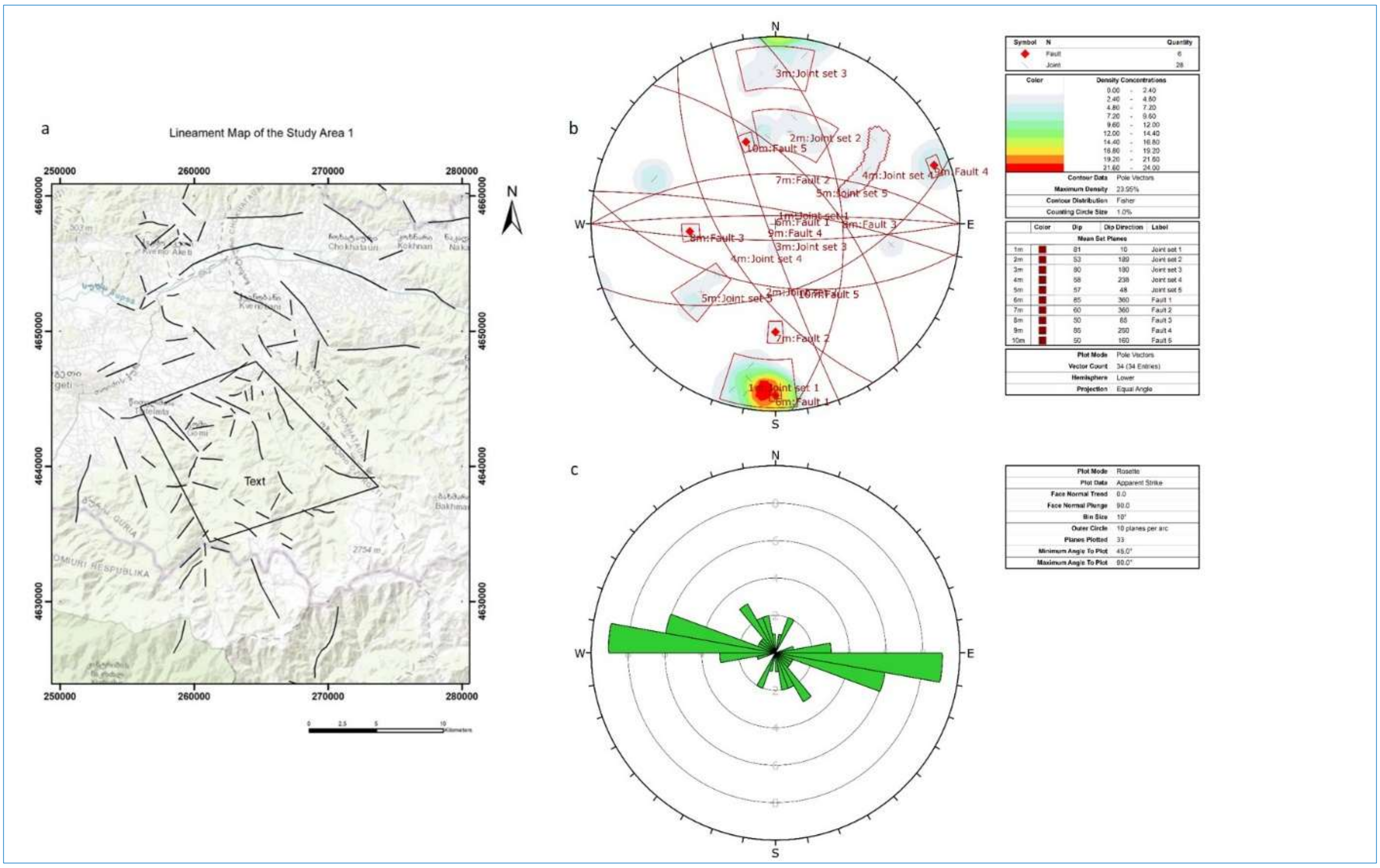


Fig. 7. Lineaments map და DIPS analyses

## 5. Conclusion

This study demonstrates that the Vakijvari ore field represents a multiphase magmatic–hydrothermal system developed within an intracontinental extensional setting. Although the geodynamic interpretation relies primarily on major-oxide geochemistry, the integration of mineralogical, petrological, and structural data consistently supports the model of magma evolution in an extensional crust during the Middle Eocene.

The intrusive rocks exhibit calc-alkaline, metaluminous to weakly peraluminous compositions and record a magmatic evolution dominated by fractional crystallization of water-rich melts. These geochemical characteristics, together with the observed mineralogical assemblages, are compatible with extensional, rift-related magmatism.

Hydrothermal alterations—including sericitization, chloritization, and kaolinitization—reflect fluid activity at low to moderate temperatures, and these zones are spatially linked to the loci of mineralization. The close association between alteration halos and ore occurrence highlights the importance of late-stage magmatic fluids in forming the mineralized system.

Structural analysis, supported by remote sensing data, shows that mineralization is preferentially concentrated at the intersection of NE–SW and NW–SE fault systems. These structural nodes acted as high-permeability zones that facilitated focused fluid flow and metal deposition. Thus, the causal relationship between magmatic differentiation, structurally controlled fluid pathways, and ore localization is clearly expressed within the Vakijvari system.

Overall, the Vakijvari ore field represents a well-preserved example of a hydrothermal mineralization system associated with intracontinental rifting. The results contribute to regional metallogenic understanding by aligning Vakijvari with similar Eocene extensional Cu-polymetallic systems documented in the Armenian Highland and Iranian post-collisional belts, where magma evolution and fault-controlled permeability similarly govern mineralization patterns. These insights provide a useful framework for exploring and predicting mineralization in structurally analogous rift-related settings.

## Acknowledgment

We express our deepest gratitude to our colleagues and friends – Dr. Birgit Mueller of the Karlsruhe Institute of Technology and Dr. Benjamin Busch, whose professional support has greatly contributed to the successful implementation of our research.

## References

Adamia, S., Chabukiani, A., Sadradze, N., Zakariadze, G. (2011). Tectonic evolution of the Caucasus region — From Gondwana to the present. Geological Society, London, Special Publications 377 (1), 261–280. https://doi.org/10.1144/SP377.11.

Adamia, S., Zakariadze, G., Chabukiani, A., Sadradze, N., Tsereteli, N., 2,010. Tectonic evolution of the Caucasus region—a brief overview. Geological Society, London, Special Publications 340 (1), 317–332. https://doi.org/10.1144/SP340.14.

Audétat, A., Günther, D., Heinrich, C.A., 2000. Causes for large-scale metal zonation around mineralized plutons: Fluid inclusion LA-ICP-MS evidence from the Mole Granite, Australia. Economic Geology 95 (8), 1563-1581. https://doi.org/10.2113/gsecongeo.95.8.1563.

Bissig, T., Tosdal, R.M., 2009. Stratigraphic controls on epithermal Au-Ag mineralization in volcanic basins: A review of the El Pechón deposit, Argentina. Economic Geology 104 (7), 1153-1168. https://doi.org/10.2113/gsecongeo.104.7.1153.

Bonin, B., 2004. Do coeval mafic and felsic magmas in post-collisional to within-plate regimes necessarily imply two contrasting mantle and crustal sources? Lithos 78 (1-2), 1-24. https://doi.org/10.1016/j.lithos.2004.04.042.

Chiaradia, M., 2009. Adakite-like magmas from a non-subduction setting: Evidence from the Miocene post-collisional volcanism in the NW Alps. Lithos 111 (1-2), 39-56. https://doi.org/10.1016/j.lithos.2008.11.001.

Chkhikvishvili, Z., 1992. Preparation of geological-geochemical-geophysical foundations for the search for gold in Guria in Guria's oral area. Unpublished Technical Report, Institute of Geology, Tbilisi.

Cooke, D.R., Hollings, P., Walshe, J.L., 2011. Giant porphyry deposits: Characteristics, distribution, and tectonic controls. Economic Geology 106 (5), 803-840. https://doi.org/10.2113/econgeo.106.5.803.

Cox, K.G., Bell, J.D., Pankhurst, R.J., 1979. The Interpretation of Igneous Rocks. London: Allen & Unwin.

Faulds, J.E., Varga, R.J., 1998. The role of accommodation zones and transfer zones in the regional segmentation of extended terranes. GSA Special Papers, 323, 1-45. https://doi.org/10.1130/0-8137-2323-X.1.

Frost, B.R., Barnes, C.G., Collins, W.J., Arculus, R.J., Ellis, D.J., Frost, C.D., 2001. A geochemical classification for granitic rocks. Journal of Petrology 42 (11), 2033–2048. https://doi.org/10.1093/petrology/42.11.2033.

Gamkrelidze, I., Okrostsvaridze, A., Koiava, K., Maisadze, F., 2020. Geological structure of Georgia. In I. Gamkrelidze (Ed.), Geological Structure of Georgia (pp. 11–24). Springer Nature. https://doi.org/10.1007/978-3-030-40704-6_2.

Ghasemi, A., Talbot, C.J., 2006. A new tectonic scenario for the Sanandaj–Sirjan Zone (Iran). Journal of Asian Earth Sciences 26 (6), 683-693. https://doi.org/10.1016/j.jseaes.2005.01.002.

Gillespie, A.R., Kahle, A.B., Walker, R.E., 1987. Color enhancement of highly correlated images: I. Decorrelation and HSI contrast stretches. Remote Sensing of Environment 20 (3), 209-235. https://doi.org/10.1016/0034-4257(87)90088-5.

Jebelli, M., Yousefi, M., 2022. Post-collisional porphyry Cu–Au mineralization in Iran: Structural controls and tectonic implications. Ore Geology Reviews 143, 104730. https://doi.org/10.1016/j.oregeorev.2021.104730.

McKenzie, D., Bickle, M.J., 1988. The volume and composition of melt generated by extension of the lithosphere. Journal of Petrology, 29(3), 625–679. https://doi.org/10.1093/petrology/29.3.625.

Middlemost, E.A.K., 1994. Naming materials in the magma/igneous rock system. Earth-Science Reviews, 37 (3–4), 215-224. https://doi.org/10.1016/0012-8252(94)90029-9.

Moritz, R., Heinrich, C.A., Petrunov, R., 2004. Late Cretaceous Cu–Au epithermal deposits of the Panagyurishte district, Srednogorie zone, Bulgaria. In Hedenquist, J.W., Thompson, J.F.H., Goldfarb, R.J., Richards, J.P. (Eds.), Economic Geology 100th Anniversary Volume 1905-2005 (pp. 1035-1059). Society of Economic Geologists. https://doi.org/10.5382/AV100.28.

Okrostsvaridze, A., Chang, I.H., Gagnidze, N., Bluashvili, D., Boichenko, G., Gogoladze, S., 2020. Zircon U–Pb geochronology and analysis of magmatic processes of ore-bearing plutons in the Achara–Trialeti rift-fold zone of the Lesser Caucasus [in Georgian]. Proceedings of the Georgian National Academy of Sciences, Series of Earth Sciences 48 (2), 123-135.

Pearce, J.A., 1996. A user's guide to basalt discrimination diagrams. In Trace Element Geochemistry of Volcanic Rocks: Applications for Massive Sulphide Exploration (pp. 79-113). Geological Association of Canada, Short Course Notes 12.

Richards, J.P., 2005. Causal links between igneous activity, mineralization, and regional tectonics. Economic Geology 100 (6), 111–118. https://doi.org/10.2113/gsecongeo.100.6.111.

Rollinson, H.R., 1993. Using Geochemical Data: Evaluation, Presentation, Interpretation. Longman.

Rowan, L.C., Mars, J.C., Simpson, C.J., 2005. Lithologic mapping of the Mordor REE–Th deposit, Australia, using ASTER data. Remote Sensing of Environment 99 (1-2), 105-126. https://doi.org/10.1016/j.rse.2004.11.021.

Shand, S.J., 1927. Eruptive Rocks. John Wiley & Sons.

Sibson, R.H., 1996. Structural permeability of fluid-driven fault-fracture meshes. Journal of Structural Geology 18 (8), 1031-1042. https://doi.org/10.1016/S0191-8141(96)00032-6.

Sillitoe, R.H., 2010. Porphyry copper systems. Economic Geology

105 (1), 3-41. https://doi.org/10.2113/gsecongeo.105.1.3.

Sisson, T.W., Grove, T.L., 1993. Experimental investigations of the role of H2O in calc-alkaline differentiation and subduction zone magmatism. Contributions to Mineralogy and Petrology 113 (2), 143-166. https://doi.org/10.1007/BF00283225.

Sosson, M., Adamia, S., Rolland, Y., 2010. Subductions, obduction and collision in the Lesser Caucasus (Armenia, Azerbaijan, Georgia): New insights. In Sosson, M., Kaymakci, N., Stephenson, R. A., Bergerat, F., Starostenko, V. (Eds.), Sedimentary basin tectonics from the Black Sea and Caucasus to the Arabian Platform. Geological Society, London, Special Publications 340 (1), 329-352. https://doi.org/10.1144/SP340.14.

White, N.C., Hedenquist, J.W., 1995. Epithermal gold deposits: Styles, characteristics and exploration. Society of Economic Geologists Newsletter 23, 1-13.

Wilson, M., 1989. Igneous Petrogenesis: A Global Tectonic Approach. London: Unwin Hyman.